

Reaction Engineering of Through-Chip Via Filling for Wafer-Level 3D Packaging

*D.P.Barkey¹, J. Callahan², A. Keigler³, Z. Liu³, A. Ruff², J. Trezza² and B. Wu³

¹University of New Hampshire

Department of Chemical Engineering, Durham NH 03824 USA

²Cubic Wafer, Inc., New Hampshire Development Center

10 Al Paul Lane, Merrimack, New Hampshire 03054

³Nexx Systems

5 Suburban Park Drive, Billerica, MA 01821-3904

Abstract

Through-chip vias, 170 microns in depth and 10 to 35 microns in diameter were filled by electrodeposition of copper. The process was optimized for reliability and speed through a combination of process modeling, electro-analytical studies and pilot scale plating on 8-inch wafers in a commercial process unit. The approach is based on use of reverse pulses and oxygen diffusers to maintain an optimum distribution of accelerator over the wafer. Results of electroanalytical studies on a rotating disk electrode (RDE) and rotating ring-disk electrode (RRDE) are presented to demonstrate quantitatively the role of transport-limited redox processes in regulating the distribution of accelerant within vias. Results of dimensional analysis and numerical simulation are presented and used to relate the electroanalytical results with the proposed mechanism. A three-hour pilot-scale plating process optimized through application of these results is demonstrated for 170 micron deep vias.

Problem and Approach

The accelerants in standard super-conformal copper-plating additive systems for cupric sulfate-sulfuric acid plating baths are precursors that form the true accelerant by reaction with Cu(I). As a result, the coupling among Cu(I), Cu(II) and O₂ plays a critical role in the additive mechanism, and both Cu(I) and dissolved oxygen must be regarded as components of the additive ensemble.[1-4]

The authors have developed an approach to these filling problems that is based on localized control of the accelerant concentration through reaction-engineering principles. The accelerant concentration can be regulated indirectly by control of the local Cu(I) concentration. There are two levers of control over Cu(I) concentration; an oxidizer, such as dissolved oxygen,[5,6] and reverse-current pulses.[2] Because dissolved oxygen can be replenished by use of a diffuser, and Cu(I) can be generated by reverse current pulses, these components of the additive ensemble can be modulated dynamically without changing out the bath or adding material.

Under the proposed hypothesis, mass transport is the rate limiting step in the generation and consumption of accelerant. In a plating machine that produces intense agitation at the wafer surface, there is a large contrast between reaction-diffusion conditions inside and outside of the vias. This difference can be exploited to produce a large ratio of current in the via to current outside the via (fill ratio), and to produce a desired gradient of deposition rate from via bottom to via opening.

The chemistries used in the present study are based on those commercially applied to formation of on-chip interconnects. Additive systems used in formation of sub-micron scale on-chip interconnects produce a superconformal current distribution so that the deposition rate is higher within recesses than on surrounding areas. Evidently, the mechanism is controlled by geometric factors.[7-10] A suppressor, such as poly(ethylene glycol) (PEG), is adsorbed onto the surface where it inhibits deposition.[11-13] An accelerant, a derivative of, for example, bis(3-sulfopropyl)disulfide or SPS, displaces or lifts the suppressor and re-activates the surface.

The filling of through-chip vias, however, cannot be understood on the basis of the curvature-driven model alone. In through-chip via filling, an enormous contrast in current density between the via interior and exterior wafer surface is maintained for periods of up to several hours and in the absence of significant curvature. Moreover, on these large time scales, one should expect the accelerant to achieve saturation of the surface, after which curvature could no longer drive its accumulation. The mechanism and analysis reported here demonstrate a rational procedure for design and execution of large-scale filling processes. These studies employed both the PEG/SPS/Cl⁻ system and a commercial formulation.

Experiment and Simulation

The reaction diffusion scheme is illustrated in Figure 1. Because the Cu(0)/Cu(I) couple is reversible, the interfacial concentration of Cu(I) is always in equilibrium with the metal and can be estimated with the Nernst equation.

During deposition at cathodic potentials, this concentration is negligible. On the reverse pulse, at positive potential, it reaches a maximum value, and then falls again during the off time. During the off-time, Cu(I) that enters the diffusion layer from the surface is consumed by reaction with oxygen diffusing in from the bulk solution. Because the accelerant is produced by

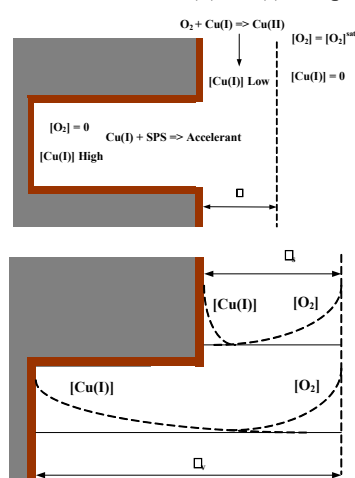


Figure 1. Reaction-diffusion model of accelerant production and consumption on a wafer surface and inside a via. Top; reaction and diffusion processes. Bottom; concentration profiles of Cu(I) and O₂ at the beginning of the off-time.

reaction of a precursor with Cu(I), the amount of Cu(I) remaining in the boundary layer at the end of the off-time determines the amount of accelerant present when the forward duty cycle begins.

A dimensional analysis based on the reaction diffusion model proceeds as follows. The boundary layer thickness on the wafer surface in the Nexx Systems wafer-plating machine is about 25 microns thick. At the bottom of the via, the equivalent boundary layer thickness is roughly 195 microns, the sum of the surface boundary layer thickness and the via depth. A numerical estimate of the diffusion time scale for transport of Cu(I) can be calculated for the wafer surface (s) and the via (v).

$$\tau_s = \frac{\delta_s^2}{4D} = \frac{(2.5 \times 10^{-4} \cdot \text{cm})^2}{4 \times 5 \times 10^{-6} \cdot \text{cm}^2 / \text{s}} \approx 0.3 \cdot \text{s}$$

$$\tau_v = \frac{\delta_v^2}{4D} = \frac{(1.95 \times 10^{-2} \cdot \text{cm})^2}{4 \times 5 \times 10^{-6} \cdot \text{cm}^2 / \text{s}} \approx 20 \cdot \text{s}$$

The Cu(I) concentration profile within the boundary layer falls into one of three regimes. At short times, less than τ , there is a transient during which the diffusion profile penetrates only a fraction of the distance into boundary layer and is well described by diffusion into a semi-infinite space. As a result, the profile is independent of boundary layer thickness. On time-scales longer than τ , oxygen arriving from the bulk solution has consumed all of the Cu(I) outside of a very short distance from the surface. In this case, the concentration of Cu(I) is also independent of boundary layer thickness. At times shorter than both τ_s and τ_v , or longer than both τ_s and τ_v , conditions inside and outside via are therefore comparable. At intermediate times, however, the two regions are in different regimes, and this intermediate time scale, between 0.3 s and 20 s, should bracket the optimum off-time for filling. For an off-time duty cycle of 50 %, the optimum wave-train frequency is therefore expected to fall in the range of 0.1 to 1.7 Hz.

Concentrations of Cu(I) at the surface, and the concentration of dissolved oxygen in the bulk solution are fixed thermodynamically. The concentration profiles in the diffusion layer are controlled by mass transport. The electroanalytical experiments used to simulate the diffusion mechanism in the vias are based on the rotating disk electrode (RDE), (see Figure 2). A high rotation speed (1800 rpm, $\delta = 25 \mu\text{m}$) is selected to simulate the environment on a wafer surface, while a low rotation speed (36 rpm, $\delta = 180 \mu\text{m}$) is selected to simulate the bottom of the via.. The potential wave-train is applied under both conditions, and the current is integrated to give the deposit charge. The ratio of charge at low rotation speed (via bottom) to that at high

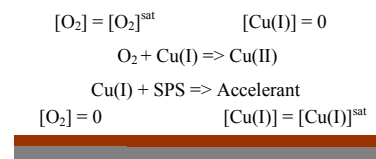


Figure 2. Reaction-diffusion process at a planar rotating disk electrode.

rotation speed (wafer surface) is called the fill ratio. A higher fill ratio predicts better filling.

In each RDE experiment, one process parameter is varied while all others are held fixed. Process parameters include additive concentrations, applied current or potential or the pulse-reverse wave-train parameters. For a fixed overall deposition rate, there are four wave-train parameters; frequency, forward duty cycle, reverse duty cycle and the difference in potential or current between the forward and reverse cycles.

In the RDE experiments, the solution was made up of 0.5 M CuSO_4 /1 M H_2SO_4 with 50 ppm Cl^- , 400 ppm PEG and 1 or 2 ppm SPS. The reference and counter electrodes were copper inserted into bridge tubes equipped with fritted glass plugs to prevent anolyte coming into contact with the plating solution. The measurements were performed under air. The pulse reverse waveform was applied with a PARC Model 2263 potentiostat under computer control through LabView.

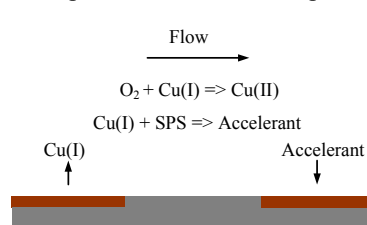


Figure 3. Reaction-diffusion process at a rotating ring disk electrode.

The kinetics of accelerant generation and destruction were studied with a rotating ring-disk electrode (RRDE). (see Figure 3). The ring was held at a constant cathodic potential while the disk was cycled between cathodic and anodic

potentials. During the anodic sweep, Cu(I) generated at the disk is convected toward the ring. Between the disk and ring, accelerant may be formed by reaction of Cu(I) with SPS or consumed by reaction with oxygen. The cell arrangement in the RRDE experiments was the same as that in the RDE experiments, except that the disk and ring were controlled with a Pine Instruments Model AFCBP1 bipotentiostat. The solution was 0.05 M CuSO_4 /1 M H_2SO_4 with 50 ppm Cl^- , 400 ppm PEG and 1 or 2 ppm SPS. A low cupric ion concentration was used in the RRDE experiments to prevent rapid area change on the ring electrode.

Pilot scale plating was carried out on wafer segments mounted on a RDE as well as on eight inch wafers plated in a commercial machine.

Results and Discussion

The RDE experiments were based on potentiostatic pulse-reverse deposition. A typical potential wave-train and current response are shown in Figures 4 and 5. In industrial operations, a galvanostatic pulse is preferred because it allows precise control of the rate of deposition and the total charge deposited. Comparison of the potentiostatic wave-train and the current response shows that potentiostatic and galvanostatic operations are similar.

For the present purposes, potentiostatic operation is preferable for simulation of the practical process. In a real plating operation, the applied current does not impose the same current density on all portions of the wafer. Instead it represents an integral of current density over the entire surface including vias. Because the seed layer is conductive,

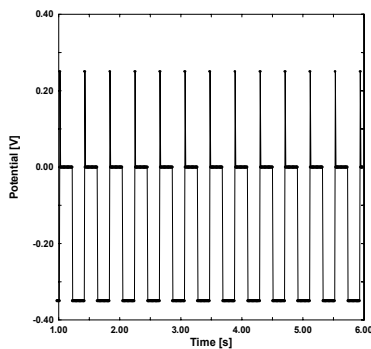


Figure 4. Potentiostatic Pulse-reverse Wave-train.

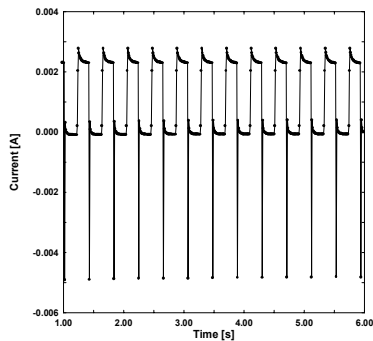


Figure 5. Galvanic response to potentiostatic pulse-reverse wave-train.

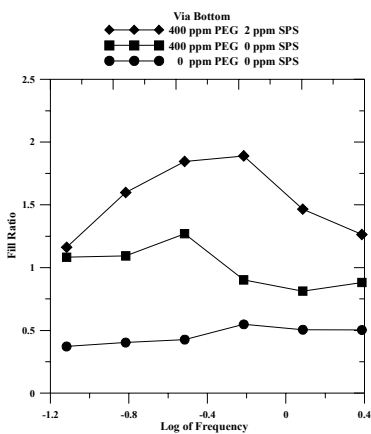


Figure 6. Frequency dependence of the fill ratio.

RDE are shown in Figures 6-9. Each of the four variables was varied independently. The basic wave form was made up of deposition at -300 mV for 400 ms, dissolution at 100 mV for 40 ms and an off-time at 0 mV vs Cu for 400 ms.

The frequency was varied while holding the applied potentials and duty cycles constant. Without additives, or with PEG only, the fill ratio was independent of frequency (see Figure 6). Addition of SPS increased the fill ratio and also produced a maximum as a function of frequency. The time scale of the maximum falls within the range predicted by the dimensional analysis. The effect is seen only in the presence of SPS, as expected based on the model.

the via bottoms and the wafer surface are more nearly at the same potential than at the same current density. By imposing a given potential at two rotation speeds, one can measure directly the contrast in current density between the two points and assess the filling power of the process.

In the experiments, the current was integrated over multiple cycles to a fixed total process time. Each change in the frequency was compensated by a corresponding change in the number of cycles to hold the process time constant from one experiment to the next. The reverse pulse charge was always negligible in comparison with the total charge passed, and each pulse corresponded to less than a monolayer of metal, so that the primary effect of the pulse is generation of Cu(I) rather than removal of surface-confined materials. The wave-train parameters that were varied were frequency, forward duty cycle, reverse duty cycle and the potential difference between forward and reverse pulse potentials.

The effects of wave-train parameters on deposition on the

The forward duty cycle was varied around the basic wave-train by variation of the plating time (i.e. 200, 400, 800 ms) and reduction of the off-time by a corresponding amount to hold the frequency constant. The forward duty cycle had no significant effect on the fill ratio (see Figure 7). A similar result was obtained for the reverse duty cycle. (see Figure 8) Evidently, the time dependent reaction diffusion processes take place during the off-time because the duration of the forward and reverse pulses had little effect on the fill ratio, whereas the frequency, and, hence the duration of the off-time, had a strong effect.

The dependence of the fill ratio on pulse potential is shown in Figure 9. The fill ratio rises very rapidly with reverse potential. The Nernst equation predicts an exponential increase in interfacial Cu(I) concentration with increasing potential and, hence, a high driving force for Cu(I) generation.

A typical RRDE (Pt-Pt) result is shown in Figure 10. The ring electrode was held at a constant cathodic potential while the disk potential was scanned through two complete cycles from a positive vertex to a negative vertex and back. The plots show the disk current (solid line) and ring current (dashed line) versus disk potential. On the negative end of the scan, the disk current shows a deposition current (negative in these plots.), and the positive end shows a stripping curve. As the disk is scanned to a negative potential, the ring current is slightly reduced as the disk consumes copper ion. In the absence of SPS, when the disk potential is scanned into the anodic region, Cu(I) and Cu(II) are generated at the disk and convected to the ring. The result is an increase in ring potential as these ions are captured. The current reverts to the

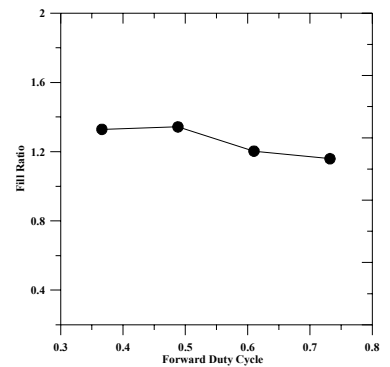


Figure 7. Dependence of the fill ratio on Forward duty cycle.

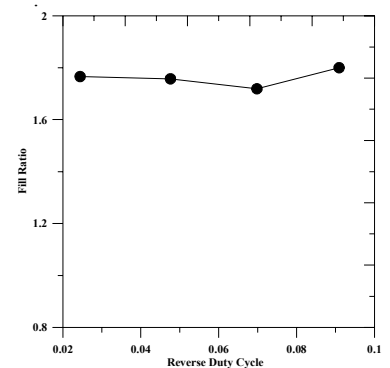


Figure 8. Dependence of the fill ratio on reverse duty cycle.

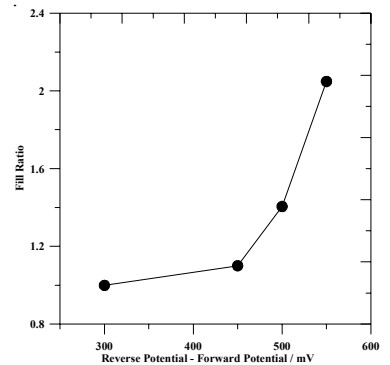


Figure 9. Dependence of the fill ratio on reverse pulse potential.

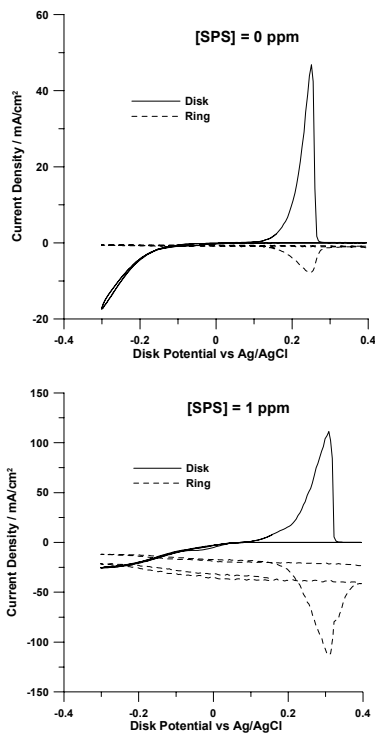


Figure 10. RRDE Curves.

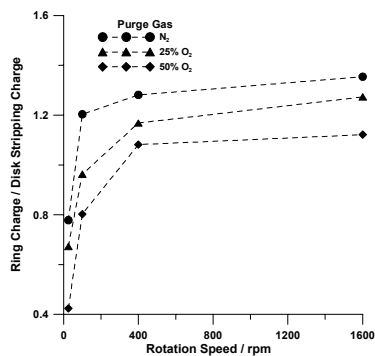


Figure 11. Excess ring charge versus RRDE rotation speed with various Purge gases.

concentration in Figure 11. At high rotation speed, there is clearly an accelerant effect. The charge ratio is in excess of one. At low rotation speed it falls off toward the collection efficiency.

This pattern can be understood by considering the process that takes place between the disk and the ring. At low rotation speed, the transit time from disk to ring is relatively large. The contact time between Cu(I) and oxygen is long and there is sufficient reaction time for destruction of Cu(I) and accelerant by oxygen. As a result and the excess ring charge is small. As the rotation speed is increased, the excess charge rises because more accelerant survives and reaches the ring. The effect of the purge gas follows the same logic. Under oxygen purge, the rate of consumption of Cu(I) and accelerant is greater because the concentration of dissolved

oxygen is higher. The dependence of accelerant effect on contact time and dissolved oxygen concentration suggests that there is a significant kinetic impedance to the process of accelerant consumption in solution.

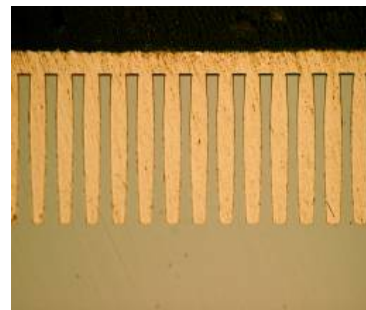
In the presence of SPS, the effect of the Cu(I) generated during disk stripping is amplified by the resulting production of accelerant. The increase in ring current is much larger, and it persists after the disk is fully stripped. Evidently, accelerant produced in response to generation of Cu(I) at the disk arrives at the ring, accelerates deposition and remains in place. The integral of the excess ring current can be compared with the collection efficiency of the RRDE, about 20%. If the excess ring current is due entirely to capture of ions generated by the stripping current, the ratio of excess ring charge to disk stripping charge should be about 0.2. If, instead, the excess ring current is due to accelerated growth induced by formation of accelerant, the ratio of excess ring charge to disk stripping charge should be larger.

This ratio is presented as a function of RRDE rotation speed and purge-gas

oxygen is higher. The dependence of accelerant effect on contact time and dissolved oxygen concentration suggests that there is a significant kinetic impedance to the process of accelerant consumption in solution.

The electroanalytical procedures described above provide a simple and rapid means of optimizing a plating process. For each process parameter, the fill ratio is measured over a range of parameter values. The optimal parameter value is the one that maximizes fill ratio.

The optimal parameters were then tested on two levels; wafer segments, six square centimeters in size mounted on rotating disk electrodes, and full eight inch wafers plated in a Nexx plating machine using a commercial additive chemistry (Enthone CuBath ViaFill). Additive concentrations and pulse parameters were optimized by the electroanalytical procedure



described above. Vias 150 to 170 microns in depth and 10 to 15 microns in diameter were successfully filled in three hours.

Figure 12. 10 X 170 micron through-chip vias filled in three hours.

Conclusions

Cu(I) produced by anodic dissolution during a reverse pulse generates free accelerant by reaction with SPS. The free accelerant is consumed homogeneously by O₂ during the off-time in a reaction-diffusion process. Surviving accelerant that reaches a surface undergoing copper deposition increases the deposition rate there. The increase is greatest within deep vias, where the accelerant is protected from contact with dissolved oxygen. Cu(I) and O₂ are properly regarded as part of the PEG-SPS-Cl- additive ensemble, and a combination of pulse-reverse current and gas purging can be employed to optimize the performance of the additive ensemble.

A procedure for screening and optimizing additive formulations and pulse-reverse wave-trains has been described. Through the use of hydrodynamic electrodes, the distribution of current between vias and wafer surfaces can be simulated in simple and rapid bench scale measurements.

Acknowledgments

This work was supported by a grant from the New Hampshire Industrial Research Center with matching funds from Cubic Wafer Inc.

References

1. K. Kondo, T. Yonezawa, D. Mikami, T. Okubo, Y. Taguchi, K. Takahashi and D. Barkey, *J. Electrochem. Soc.*, 152, H173 (2005).
2. D. Barkey, F. Oberholtzer and Q. Wu, *J. Electrochem. Soc.*, 145, 590 (1998).
3. D. Hua and D. Barkey, *Plat. & Surf. Finish.*, 90, 40 (2003)
4. P.M. Vereecken, R.A. Binstead, H. Deglianni and P.C Andricacos, *IBM J. Res & Dev.*, 49, 3, (2005).

5. Frank and A.J. Bard, *J. Electrochem. Soc.*, 150, C244 (2003)
6. K. Kondo, N. Yamakawa, Z. Tanaka and K. Hayashi, *J. Electroanal. Chem.*, 559, 137 (2003).
7. T.P.Moffat, J.E.Bonevich, W.H.Huber. A.Stanischevsky, D.R.Kelly G.R.Stafford and D. Josell, *J. Electrochem. Soc.*, 147, 4524 (2000)
8. A.C. West, S. Mayer and J. Reid, *Electrochem. Solid-State Lett.*, 4, C50 (2001)
9. M.L. Walker, L.J. Richter and T.P. Moffat, *J. Electrochem. Soc.*, 153 C557 (2006)
10. D. Josell, D. Wheeler, W.H. Huber and T.P. Moffat, *Phys. Rev. Lett.*, 87, 1 (2001).
11. Y. Jin, K. Kondo, Y. Suzuki, T. Matsumoto and D. Barkey, *Electrochem. Solid State Lett.*, 8, C6 (2005)
12. J.P. Healy, D. Pletcher, M. Goodenough, *J. Electroanal. Chem.*, 338, 155 (1992)
13. K.R. Hebert, *J. Electrochem. Soc.*, 148, C726 (2001)